

# N-Cadherin Prodomain Cleavage Regulates Synapse Formation *In Vivo*

Nazlie S. Latefi, Liliana Pedraza, Anne Schohl, Ziwei Li, Edward S. Ruthazer

McGill Program in NeuroEngineering, Department of Neurology and Neurosurgery,  
Montreal Neurological Institute, McGill University, Montreal, Quebec, Canada H3A 2B4

Received 30 November 2008; revised 20 February 2009; accepted 21 February 2009

**ABSTRACT:** Cadherins are initially synthesized bearing a prodomain that is thought to limit adhesion during early stages of biosynthesis. Functional cadherins lack this prodomain, raising the intriguing possibility that cells may utilize prodomain cleavage as a means to temporally or spatially regulate adhesion after delivery of cadherin to the cell surface. In support of this idea, immunostaining for the prodomain of zebrafish N-cadherin revealed enriched labeling at neuronal surfaces at the soma and along axonal processes. To determine whether post-translational cleavage of the prodomain affects synapse formation, we imaged Rohon-Beard cells in zebrafish embryos expressing GFP-tagged wild-type N-cadherin (NCAD-GFP) or a GFP-tagged N-cadherin mutant

expressing an uncleavable prodomain (PRON-GFP) rendering it nonadhesive. NCAD-GFP accumulated at synaptic microdomains in a developmentally regulated manner, and its overexpression transiently accelerated synapse formation. PRON-GFP was much more diffusely distributed along the axon and its overexpression delayed synapse formation. Our results support the notion that N-cadherin serves to stabilize pre- to postsynaptic contacts early in synapse development and suggests that regulated cleavage of the N-cadherin prodomain may be a mechanism by which the kinetics of synaptogenesis are regulated.

© 2009 Wiley Periodicals, Inc. *Develop Neurobiol* 00: 000–000, 2009

**Keywords:** cadherin; zebrafish; Rohon-Beard; synaptogenesis; prodomain

## INTRODUCTION

Adhesive interactions between the pre- and postsynaptic membranes have been proposed to participate in the formation and maturation of the synapse (Sperry, 1963; Vaughn, 1989; Fannon and Colman, 1996; Benson and Tanaka, 1998; Craig and Lichtman, 2001; Lohmann and Bonhoeffer, 2008). The homophilic cell adhesion molecule N-cadherin is present at developing synapses where it can participate in their normal maturation (Benson and Tanaka, 1998; Togashi et al., 2002). A known constituent of

presynaptic transport vesicles, which carry elements of presynaptic machinery to developing synaptic sites (Zhai et al., 2001), N-cadherin is thought to promote early synapse formation and stabilization based on studies showing a reduction in presynaptic bouton density with expression of dominant-negative N-cadherin lacking its extracellular domain (Bozdagi et al., 2000; Togashi et al., 2002). N-cadherin also participates in activity-dependent synaptic plasticity mechanisms such as long-term potentiation (Tang et al., 1998; Bozdagi et al., 2000). N-cadherin adhesion and localization could help establish stable trans-synaptic cell-cell adhesion for the localized recruitment of presynaptic vesicles, other synaptic components, and through its interaction with actin to engage the cytoskeleton in synaptic development.

The ability of a nascent axo-dendritic contact to induce synapse formation depends to a large extent on the types of signaling and adhesion molecules present pre- and postsynaptically and on the extent to

Additional Supporting Information may be found in the online version of this article.

Correspondence to: E.S. Ruthazer (edward.ruthazer@mcgill.ca).

Contract grant sponsor: NIH; contract grant number: 204839.

Contract grant sponsors: March of Dimes, NARSAD, CIHR, McGill NeuroEngineering Initiative.

© 2009 Wiley Periodicals, Inc.

Published online in Wiley InterScience(www.interscience.wiley.com).

DOI 10.1002/dneu.20718

which those molecules interact (Togashi et al., 2002; Yamagata et al., 2003; Gerrow and El-Husseini, 2006). In addition to regulation of the complement and localization of adhesion molecules at the cell surface, post-translational modification of cell adhesion molecules is another useful mechanism by which cell-cell interactions can be modulated. Regulated cleavage at the cell surface of the ectodomains of guidance and adhesion molecules by extracellular sheddases, including matrix and membrane metalloproteases, has been described as a means of regulating signaling by eliminating their ability to bind ligand (Galko and Tessier-Lavigne, 2000; Kalus et al., 2003, 2006; Reiss et al., 2005).

Cadherins are synthesized as a precursor molecule (Pre-Pro-cadherin) (Ozawa and Kemler, 1990). After cleavage of the presequence in the rough endoplasmic reticulum, the still immature pro-N-cadherin lacks adhesive properties due to steric hindrance of calcium chelating tryptophan side chains in its extracellular domain (Koch et al., 2004). Prodomain cleavage had originally been thought to occur solely intracellularly before transport to the cell surface, however biotinylation studies in cultured hippocampal neurons (Reines et al., Soc for Neuroscience Abstracts 2005; Fields, 2006) revealed that endogenous pro-N-cadherin is targeted to the cell surface and that cleavage of the prodomain occurs at the cell surface in neurons in a time frame coincident with the onset of synaptogenesis (7–10 days *in vitro*). The delivery of unprocessed N-cadherin to the cell surface could therefore constitute an endogenous dominant-negative mechanism used by neurons to regulate synapse formation during development by restricting N-cadherin-mediated adhesion.

The Rohon-Beard cell, a transient sensory cell found in the developing zebrafish spinal cord, provides an excellent experimental model for imaging synaptogenesis *in vivo* as these cells extend a single, simple central axon along the rostrocaudal axis of the spinal cord forming synaptic contacts at regular intervals. Live-cell imaging of N-cadherin in a growing Rohon-Beard axon show it to have a highly punctate expression pattern and to travel along the axon in what appear to be transport vesicles. The rate at which these vesicles accumulate into stable, nonmotile puncta is similar to the rate at which VAMP-containing vesicles accumulate into stable complexes presumed to be synapses (Jontes et al., 2004). These observations are consistent with a model in which adhesion between pre- and postsynaptic membranes favors the recruitment of synaptic components to particular locations along an axonal segment (Ziv and Garner, 2004).

Here, we present evidence that post-translational processing of N-cadherin is a potential mechanism for regulating the rate of synaptogenesis. First, we demonstrate by immunohistochemistry that endogenous pro-N-cadherin is present at distal axon terminals where it can participate in the regulation of synaptogenesis. We then show that an uncleavable form of pro-N-cadherin is not adhesive and fails to become clustered into punctate microdomains along the Rohon-Beard axon. Finally, we provide evidence that prodomain cleavage can regulate the rate of synaptogenesis in Rohon-Beard neurons *in vivo*.

## METHODS

### Plasmids

A driver plasmid containing a Gal4 sequence downstream of an Islet-1 promoter/enhancer sequence and an effector plasmid containing zebrafish NCAD-GFP downstream of an upstream activating sequence were provided by Steven Smith, Stanford University and James Jontes, Ohio State University (Jontes et al., 2004). A mutation in the zebrafish N-cadherin prodomain (amino acids 142–145) was made by site-directed mutagenesis to convert the prodomain cleavage site into a FactorXa cleavage site using the quick change site-directed mutagenesis kit (Stratagene, La Jolla, CA). The mutagenesis was performed in two steps—deletion followed by insertion. The following oligonucleotide primers (complementary to the leading strand and lagging strand, respectively) were used to delete amino acids 142–146 (corresponding to nucleotide sequence 5'-AAT CGC GTG AAA AGA-3'): 5'-GGG CGA CGA CAG TGT GGA CTG GGT CAT TCC-3' and 5'-GGA ATG ACC CAG TCC ACA CTG TCG TCG CCC-3'. The following oligonucleotide primers (complementary to the leading strand and lagging strand, respectively) were used to insert the mutated sequence: 5'-GGG CGA CGA CAG TGT GCA GAT CGA GGG AAG AGA CTG GGT CAT TCC-3' and 5'-GGA ATG ACC CAG TCT CTT CCC TCG ATC TGC ACA CTG TCG TCG CCC-3'. The mutated sequence consisted of the following nucleotides: 5'-CAG AUC GAG GGA AGA-3'. To construct a plasmid driving expression of DsRed, the CMV promoter was removed from the DsRed vector pDsRed2-N1 (Clontech, Mountain View, CA).

The UAS was excised from the NCAD-GFP driver plasmid and subcloned into the multiple cloning site of the DsRed vector following removal of the pDsRed2-N1 CMV promoter.

### Injection and Mounting of Zebrafish Embryos

Wild-type zebrafish between 6 and 12 months of age were provided by Dr. Pierre Drapeau (University of Montreal) and purchased from the Zebrafish International Resource

Center (WIK strain) (Eugene, OR), maintained in an Aquaneering (San Diego, CA) flow-through aquatics system, and used for mating. Fertilized zebrafish oocytes were collected from mating tanks and placed in specialized injection trays. Using a SZX12 dissection microscope (Olympus) and PV830 Pneumatic Picopump (WPI, Sarasota, FL), a solution containing driver and effector plasmids dissolved in 0.2M KCl was pressure injected into embryos at the 2–4 cell stage. Plasmid DNA was injected at a concentration of 25 ng/ $\mu$ L of activator plasmid and 25 ng/ $\mu$ L of effector plasmid. Approximately 1/5 of cell volume was injected into the cells through the yolk.

Embryos were screened for mosaic expression ~24 h after injection. Embryos selected for analysis were anesthetized in 0.02% MS222 dissolved in a solution of 60- $\mu$ g/mL Instant Ocean (Ontario, Canada). Anesthetized embryos were then embedded in low melting point agarose (Type IX-A, Sigma-Aldrich) while in a 0.085–0.13 mm cover glass bottom Petri dishes (MatTek, Ashland MA). The agarose was allowed to solidify and then the embedded fish was immersed in 60  $\mu$ g/mL Instant Ocean containing 0.02% MS222. The immobilized embryos were then mounted for confocal analysis.

### Imaging Parameters and Analysis

Imaging of L-cells for the adhesion assay was done using an Olympus CK2 brightfield microscope equipped with a 10X air objective (0.25 n.a.).

All fluorescence images of zebrafish and histological sections were acquired on an Olympus Fluoview 1000 laser scanning confocal microscope using either a 20X (0.75 n.a.) air objective or a 60X (1.2 n.a.) water immersion objective. Optical sections in the Z- dimension were collected at intervals of 0.3  $\mu$ m. For time-lapse images, time between acquisitions of Z-stacks was 3–4 min. When imaging multiple fluorophores, sequential scanning was used. To image EGFP fluorescence, the excitation wavelength was set to 488 nm and the emission bandpass filters were set to 500–530 nm. To image Alexa 594 fluorescence, the excitation wavelength was set to 543 nm and the emission bandpass filters to 555–625 nm. To image Alexa 647-conjugated secondary antibody fluorescence, the excitation wavelength was set to 633 nm and the emission longpass filters to 664 nm. Colocalization of SV2 and PSD95 puncta in confocal images was performed using Imaris imaging analysis software Bitplane Zurich, Switzerland). Colocalization was assessed in single optical sections and verified by three-dimensional volume reconstruction. To measure sizes of individual puncta, images were loaded into Imaris imaging analysis software and puncta were measured in single optical sections at their largest diameters.

### Whole-Mount Immunocytochemistry

Larvae to be analyzed were anesthetized in 0.02% MS222 and then fixed in a solution of 0.1M phosphate buffer (PB, pH 7.4) containing 4% paraformaldehyde (PFA) and 4% sucrose overnight at 4°C. After fixation, larvae were

washed extensively in 0.1M PB, pH 7.4 with 0.3% TritonX-100 and then immersed in blocking solution (0.1M PB, pH 7.4 containing 5% normal goat serum (NGS), 4% bovine serum albumin (BSA), 1% NP40, and 0.3% Tween) overnight at 4°C. Incubation with primary antibody was also carried out overnight at 4°C. N-cadherin antibody (Ab 1221) was purchased from Abcam (Cambridge, MA) and used at a concentration of 1:200 diluted in blocking solution. Zn-12 (supernatant) was purchased from the University of Iowa Hybridoma Facility and used at a concentration of 1:250 diluted in blocking solution. SV2 antibody (ascites) was purchased from the University of Iowa Hybridoma facility and used at a concentration of 1:1000 diluted in blocking solution. PSD-95 antibody (Ab 18258) was purchased from Abcam (Cambridge, MA) and used at a concentration of 1:1000. Species-specific goat antibodies conjugated to either Alexa-488, Alexa-594, or Alexa-647 were purchased from Molecular Probes (Invitrogen). Secondary antibodies were diluted 1:500 in blocking solution and incubated overnight at 4°C. After extensive washing in 0.1M PB/0.3% Triton-X, and then 0.1M PB, larvae were mounted in mounting media (Prolong, Invitrogen) and imaged.

### Zebrafish Culture Immunocytochemistry

Cultures were prepared according to the method of Andersen (2002) and grown on Matrigel (BD Biosciences) coated cover slips for 30 h. Cells were washed twice in PBS prior to fixation for 10 min in fresh 4% PFA in PBS, followed by another 5 min in PFA ( $\pm$  0.5% Triton-X100 for permeabilized condition), and washed twice in PBS. After 1 h in a blocking solution of 10% NGS +2% BSA in PBS ( $\pm$  0.1% Tween-20 for permeabilized condition), primary antibody mixture consisting of mouse anti-tubulin (1:100, E7-S, Developmental Studies Hybridoma Bank) and rabbit anti-ProN (1:500) in blocking solution ( $\pm$  0.1% Tween-20) was applied for a 2 h incubation. Following four 5-min washes in PBS ( $\pm$  0.1% Tween-20), secondary antibodies mixture consisting of Alexa555-conjugated goat anti-mouse (1:150) and Alexa633-conjugated goat anti-rabbit (1:150) in blocking solution was applied for a 1 h incubation and then rinsed four times for 5 min in PBS and mounted on glass slides in mounting medium (Dako).

### Adhesion Assay

NCAD and PRON were cloned out of their respective vectors (above) and into pEGFP-N1 vectors (Clontech, Mountain View, CA) driven by CMV promoters. The constructs were transfected by lipofection (Superfect, Qiagen) into L-cells. Colonies of positively expressing cells were then selected and stable transfectants created for use in the adhesion assay. For the adhesion assay, L-cells were temporarily held in suspension with media HCMF containing Ca<sup>2+</sup> (0.15M). Cells were qualitatively and quantitatively assessed for aggregate formation. For the quantitative analysis, 100  $\mu$ L of cell-bearing medium was removed every 10 min the cells therein counted in a hemacytometer. Aggregates were each counted as one

entity. Percent aggregation was calculated based on the following formula:  $[(\text{count at time } 0 - \text{count at time } t) / \text{cell count at time } 0] * 100$ . In selecting colonies for passage, care was taken to select NCAD-GFP or PRON-GFP colonies with comparable levels of expression.

### NPro Antibody Generation

A region of cDNA encoding the first 130 amino acids of zebrafish N-cadherin (accession number AF418565) was amplified by PCR and then subcloned into the PQE<sub>30</sub> expression vector supplied by the Qiaexpress Type IV kit (Qiagen). Subcloned vector DNA was then used to transform M15 (pREP4) competent cells also supplied by the Qiaexpress Type IV kit. Bacterial colonies were screened for positive expression of the NPro-His tagged peptide using an anti-His antibody. High-yield cultures were then generated from this clone and protein expression induced. His-tagged NPro was purified by passing protein purified from the cultures through Ni-NT agarose columns (Qiagen). Purified NPro peptide was then sent to Covance (Denver, Pa) for polyclonal antibody production. Sera were sequentially tested for reactivity as they arrived by western blot analysis using adult zebrafish brain lysates. The most highly reactive sera were used in subsequent studies and for immunohistochemical analysis.

### Western Blot Analysis

Adult male zebrafish (3 cm in length and 7 months of age) were anesthetized in 0.02% MS222 and then placed on ice until immobile. They were rapidly decapitated and their extracted brains immersed in RIPA buffer (Pierce). Using a hand-held mortar, each brain was homogenized in 500  $\mu$ L of RIPA buffer. Protein concentration was determined by the Bradford method. 10  $\mu$ g of total protein was loaded onto each lane of a 5–20% gradient gel. After separation by SDS PAGE, proteins were transferred to nitrocellulose membranes and subjected to western blot analysis. Membranes were blocked in 5% dry milk in TBST (0.1% Tween) overnight at 4°C. Preimmune sera and immune sera were diluted in blocking solution at a concentration of 1: 20,000. Membranes were incubated in primary antibody 2 h at room temperature and then washed extensively in TBS containing 0.3% Tween. Membranes were then incubated in rabbit-specific secondary antibody (conjugated to HRP) diluted 1:4000 in blocking solution for 1 h at room temperature. Following incubation with secondary antibody, membranes were washed extensively in tris-buffered saline containing 0.3% Tween and then subjected to chemiluminescent detection. Membranes and immune sera subject to antigen competition were treated as described above except that 2 mg/mL of antigen was diluted 1:100 into blocking solution containing immune sera for 30 min at room temperature before incubating with the membrane.

All procedures were approved by the MNI Animal Care Committee in accordance with the guidelines of the Canadian Council on Animal Care.

## RESULTS

### Pro-N-Cadherin is Endogenously Expressed in the Axons of Rohon-Beard Neurons

The zebrafish was chosen as our model system because its transparency, ease of genetic manipulation, and short gestation times lend themselves to studying neuronal development *in vivo*. Also, the localization and arborization patterns of many neurons in the zebrafish central nervous system have been delineated and are highly consistent from one organism to another. The Rohon-Beard cell in particular is a large, easily identifiable sensory cell with projections in both the central and peripheral nervous systems.

First we asked whether any uncleaved N-cadherin still bearing its prodomain is normally trafficked to the cell surface to sites where it could participate in regulating synapse formation. To this end, we performed wholemount immunohistochemistry on zebrafish larvae, labeling them with the Rohon-Beard specific antibody Zn-12, and either an N-cadherin antibody (AbCAM) or a Pro-N-cadherin antibody. The Pro-N-cadherin antibody was prepared by immunizing rabbits against a peptide consisting of the first 130 amino acids of N-cadherin. Western blot analysis showed this antibody to be specific for a 150 kD protein consistent with full-length N-cadherin and a 20 kD protein (expected size of the cleaved N-cadherin prodomain). Antigen competition successfully eliminated recognition of these bands, and preimmune sera were not reactive for these proteins [Fig. 1(A)].

Staining of N-cadherin and Pro-N-cadherin is present in the perinuclear region of the Rohon-Beard neurons, but surprisingly also near the surface of the cell somata and along their axons [Fig. 1(B)]. This staining pattern is consistent with uncleaved Pro-N-cadherin being transported to the cell surface *in vivo*. It suggests that during this period of development when neuronal connectivity is being established in the spinal cord, immature Pro-N-cadherin is not exclusively found in early protein processing compartments of the cell, but appears in fact be transported out to distal processes of the axon.

To test more directly whether Pro-N-cadherin is present at the cell surface of neurons, we performed immunocytochemistry on dissociated cultured zebrafish neurons using nonpermeabilizing conditions to maintain the cell membrane intact to label surface proteins. After 30h *in vitro* many neurons extending long neurites tipped with growth cones were apparent in phase contrast images [Fig. 1(C)]. Cultures were double immunostained with the Pro-N-cadherin antibody and a

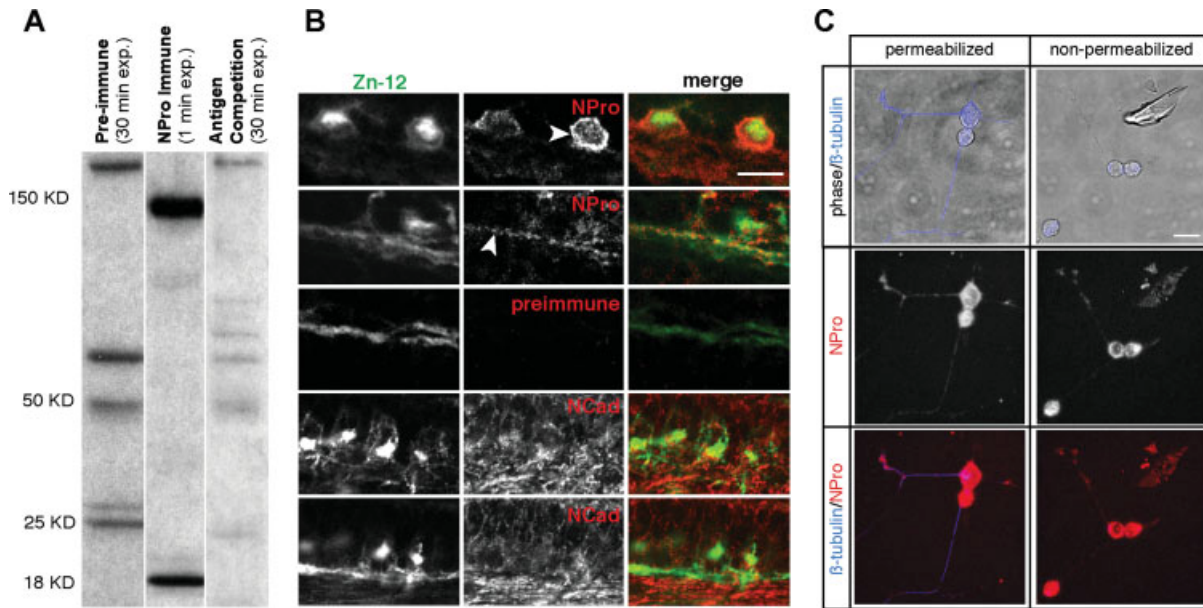


**Figure 1** NPro is expressed on the surface of Rohon-Beard cells and along axons. A polyclonal antibody generated against the prodomain of zebrafish N-cadherin (NPro) showed a high degree of specificity for NPro. (A) Western blot analysis was performed using whole adult zebrafish brain lysates. Lanes were incubated in either preimmune sera, immune sera, or immune sera that had been incubated with NPro antigen before being exposed to the membrane. Specific bands at 150 KD (expected size of uncleaved pro-N-cadherin) and 18 KD (expected size of the cleaved NPro) in the lane labeled with immune sera are absent from lanes labeled with antigen-competed immune sera or with preimmune sera even with much longer exposure times. (B) Wholemount immunohistochemistry was performed on young (24–36 hpf) zebrafish embryos. Images from a representative 30 hpf embryo are shown here. Embryos were double-labeled with a Zn-12 antibody that recognizes Rohon-Beard neurons and either NPro immune serum (top), preimmune serum (middle), or an NCAD antibody (bottom). Images are single laser scanning confocal optical sections selected to demonstrate somatic (row 1) or axonal (row 2) labeling. Arrowhead points to labeling on or near the surface of a Rohon-Beard cell body and along the axon. (C) Immunocytochemistry of cultured zebrafish neurons shows NPro staining (red in bottom panels) all along neurites and at growth cones under both permeabilized and nonpermeabilized conditions. The integrity of the cell membrane in nonpermeabilized conditions is confirmed by the absence of  $\beta$ -tubulin immunostaining (blue) in neurites revealed in overlaid phase contrast images (top). Scale bars are 10  $\mu$ m.

control  $\beta$ -tubulin antibody that labels neurites only under permeabilizing conditions. Robust Pro-N-cadherin immunoreactivity was present all along the neurites and growth cones of nonpermeabilized cells, clearly demonstrating cell surface expression of Pro-N-cadherin on the distal processes of neurons.

### Expression of N-Cadherin-GFP and Pro-N-Cadherin-GFP in Rohon-Beard Neurons

Jontes et al. (2004) provided the first *in vivo* account of synaptic cell adhesion molecule trafficking by expressing GFP-tagged N-cadherin in zebrafish Rohon-Beard neurons. Their results clearly demonstrate that N-cadherin is trafficked along the axon in

vesicles and that the extracellular domain, which mediates cadherin adhesion, is required for proper localization. When this domain is deleted, N-cadherin is no longer observed to form discrete puncta.

To determine whether the presence of the prodomain affects N-cadherin targeting within the Rohon-Beard axon, we engineered a mutant form of zebrafish N-cadherin in which the prodomain cleavage site was mutated to a FactorXa cleavage site that is not endogenously cleavable in the CNS [Fig. 2(A)] (Ozawa and Kemler, 1990; Koch et al., 2004). N-cadherin-GFP (NCAD-GFP) and Pro-N-cadherin-GFP (PRON-GFP) were expressed in Rohon-Beard neurons using the Gal4-UAS system. Two plasmids, one containing a segment of the Islet 1 promoter that selectively drives expression in Rohon-Beard cells

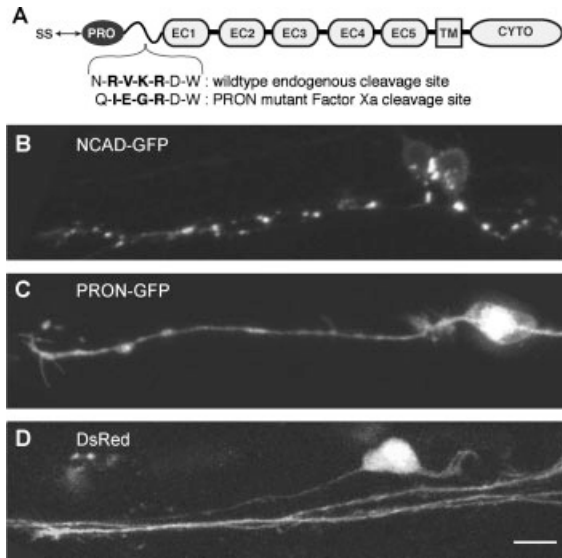


**Figure 2** NCAD-GFP, but not PRON-GFP, aggregates at microdomains along the Rohon-Beard axon. (A) Schematic of sequence domains in N-cadherin and the mutation made in the prodomain cleavage site to generate the PRON construct: SS is the signal sequence; PRO refers to the prodomain; ECD 1–5 refer to extracellular cadherin domains 1–5, respectively; TM is the transmembrane domain and cyto refers to the cytoplasmic domain. A mutation in the amino acid sequences shown made the PRON construct uncleavable endogenously but cleavable by Factor Xa. (B) NCAD-GFP expressed in a living Rohon-Beard cell is distributed in distinct punctate structures of various sizes along the axon. (C) PRON-GFP expressed in a living Rohon-Beard neuron is much more diffusely distributed. (D) Expression of DsRed as a control. As expected, the DsRed fills the cell uniformly. Images in B, C, and D are z-projections of confocal images. In all images, dorsal is toward the top. Rohon-Beard central axons and cell bodies are shown. The central axon runs axially along the spinal cord. Scale bar is 10  $\mu\text{m}$ .

driving GAL4 and another containing an upstream activating sequence driving either NCAD-GFP, PRON-GFP, or DsRed were injected into 1–4 cell stage zebrafish embryos. Between 24 and 60 h post-fertilization, live imaging was performed on a laser-scanning confocal microscope.

Time-lapse images reveal that NCAD-GFP expressed in Rohon-Beard neurons forms discrete puncta along the central axon of the cell, whereas PRON-GFP does not [Fig. 2(B,C)]. NCAD-GFP appears to be almost entirely localized to specific microdomains along the length of the axon, whereas PRON-GFP is more diffusely distributed at all ages studied. Some of the discrete NCAD-GFP puncta were motile whereas others were nonmotile. These

Developmental Neurobiology

are likely to represent active zone precursor vesicles and synaptic microdomains, respectively.

### NCAD-GFP Punctum Distribution and Dynamics Change as Rohon-Beard Axons Mature

From 1 to 2 days post-fertilization most Rohon-Beard neurons have reached their targets and are fully functional sensory cells. Time-lapse images of young (24–36 hpf) Rohon-Beard neurons expressing NCAD-GFP reveal it to be distributed along the axon in either discrete punctate structures or more diffuse, elongated tubovesicular structures [Fig. 3(A–E)]. In our observations, as Rohon-Beard neurons matured, most of the discrete puncta grew noticeably larger, the density of puncta along the axon decreased, and the tubovesicular structures became harder to detect [Fig. 3(F–J)]. These changes are evident as one compares punctum size, distribution and motility in young (24–36 hpf) and mature (36–60 hpf) Rohon-Beard neurons (Supporting Information Movies 1 and 2).

We quantitated these changes as a 79% increase in punctum diameter as Rohon-Beard neurons matured (young:  $1.21 \pm 0.22 \mu\text{m}$  and mature:  $2.16 \pm 0.32 \mu\text{m}$ ), and a 48% decrease in the density of NCAD-GFP puncta per unit length axon as Rohon-Beard neurons matured (young:  $0.18 \pm 0.03 \text{ puncta}/\mu\text{m}$  and mature:  $0.1 \pm 0.01 \text{ puncta}/\mu\text{m}$ ) [Fig. 3(K,L)]. There was also a substantial decrease in punctum motility from 1 to 2 days post-fertilization. Punctum motility was defined as puncta being displaced a distance of at least one-half their diameter within two time-lapse frames ( $\sim 8 \text{ min}$ ). As Rohon-Beard neurons matured, the number of motile puncta per axon decreased significantly: in young neurons 87.8%  $\pm$  0.5% of puncta were motile, whereas in mature neurons, only 23.4%  $\pm$  15.1% of puncta were motile [Fig. 3(M–O)]. We interpret the concomitant increase in punctum size, decrease in punctum density, and decrease in punctum motility to imply that small, motile puncta become incorporated into restricted microdomains along the axon as it matures. In Fig. 3(A–E), small puncta can be seen fusing to one another and accumulating at microdomains.

### Preventing Zebrafish N-Cadherin Prodomain Cleavage Renders it Nonadhesive

Prior studies have shown that cleavage of the prodomain of murine cadherin is necessary for its adhesive function (Ozawa and Kemler, 1990; Koch et al., 2004). We confirmed this for zebrafish N-cadherin by per-

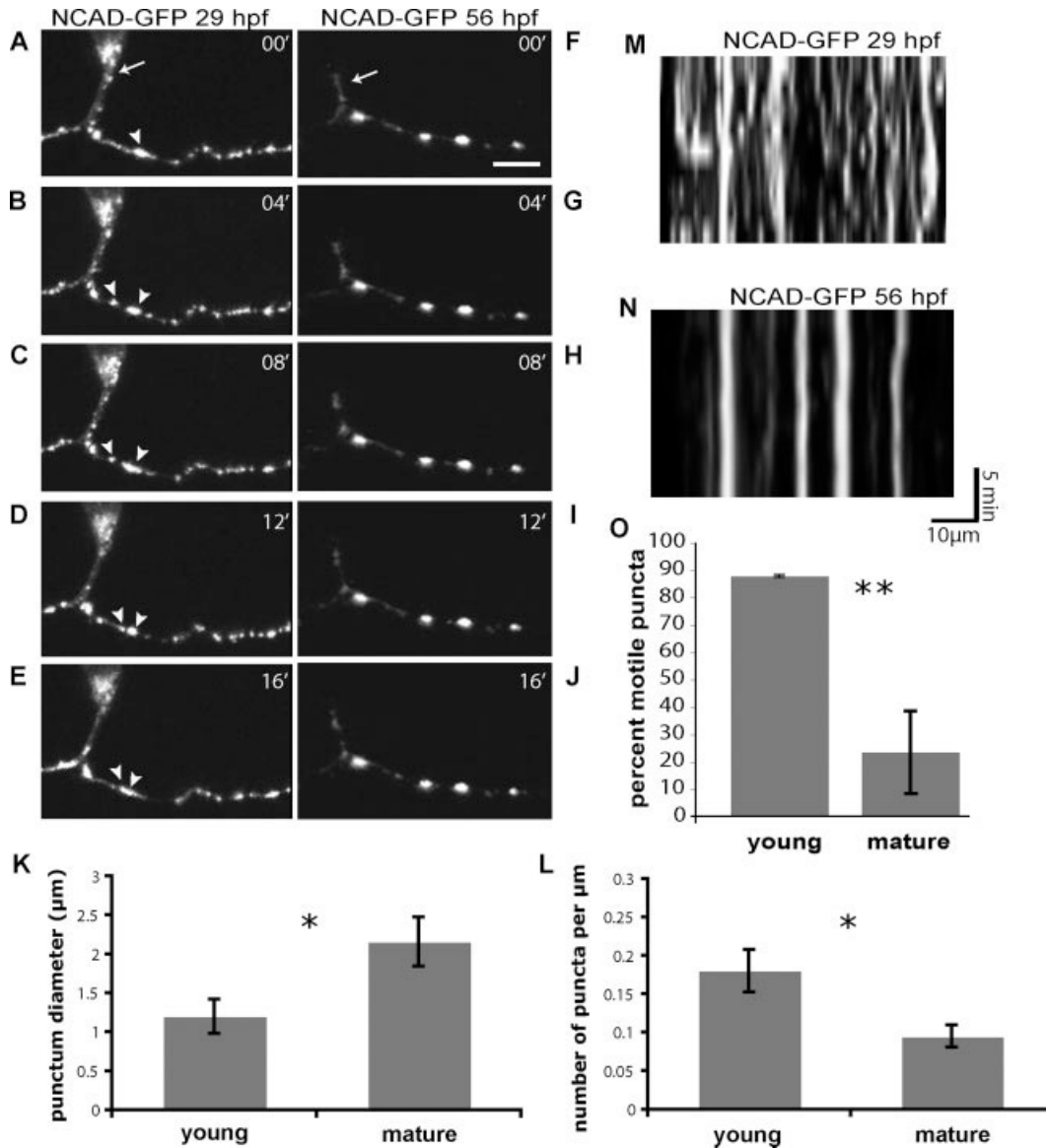


**Figure 3** NCAD-GFP puncta in Rohon-Beard neurons become larger and less motile as neurons mature. (A–E) NCAD-GFP expression at 29 hpf. NCAD-GFP puncta are numerous and of diverse sizes. Most puncta in young neurons change shape or position from one frame to the next or within two successive frames of the time-lapse experiment (time shown in minutes). Arrowhead points to a motile punctum that can be seen fusing to the larger punctum beside it over time. (F–J) By 56 hpf, most NCAD-GFP puncta are larger and nonmotile. The arrow points to the cell body of the neuron. (K, L) Puncta were smaller and more numerous in young (24–36 hpf) Rohon-Beard axons compared with mature (36–60 hpf) cells, consistent with accumulation into cadherin microdomains over time ( $N = 5$  young neurons,  $N = 8$  mature neurons). (O) Fewer motile puncta are observed as cells mature ( $N = 5$  young and 4 mature Rohon-Beard neurons). Kymographs of punctum movement in young (A–E) and mature (F–J) neurons are shown in (M) and (N), respectively. Scale bar in (F) is  $10 \mu\text{m}$ . \* $p$ , 0.05, \*\* $p$  < 0.01 Student's  $t$ -test. Error bars are SEM.

forming an *in vitro* adhesion assay (Tamura et al., 1998; Shan et al., 2000) with cells expressing either wild-type zebrafish NCAD-GFP or mutant zebrafish PRON-GFP (see Fig. 4).

Stably transfected cell lines were created in which either NCAD-GFP, or PRON-GFP was expressed in L-cells. L-cells are fibroblast-like cells that do not express cadherins endogenously and are not adhesive

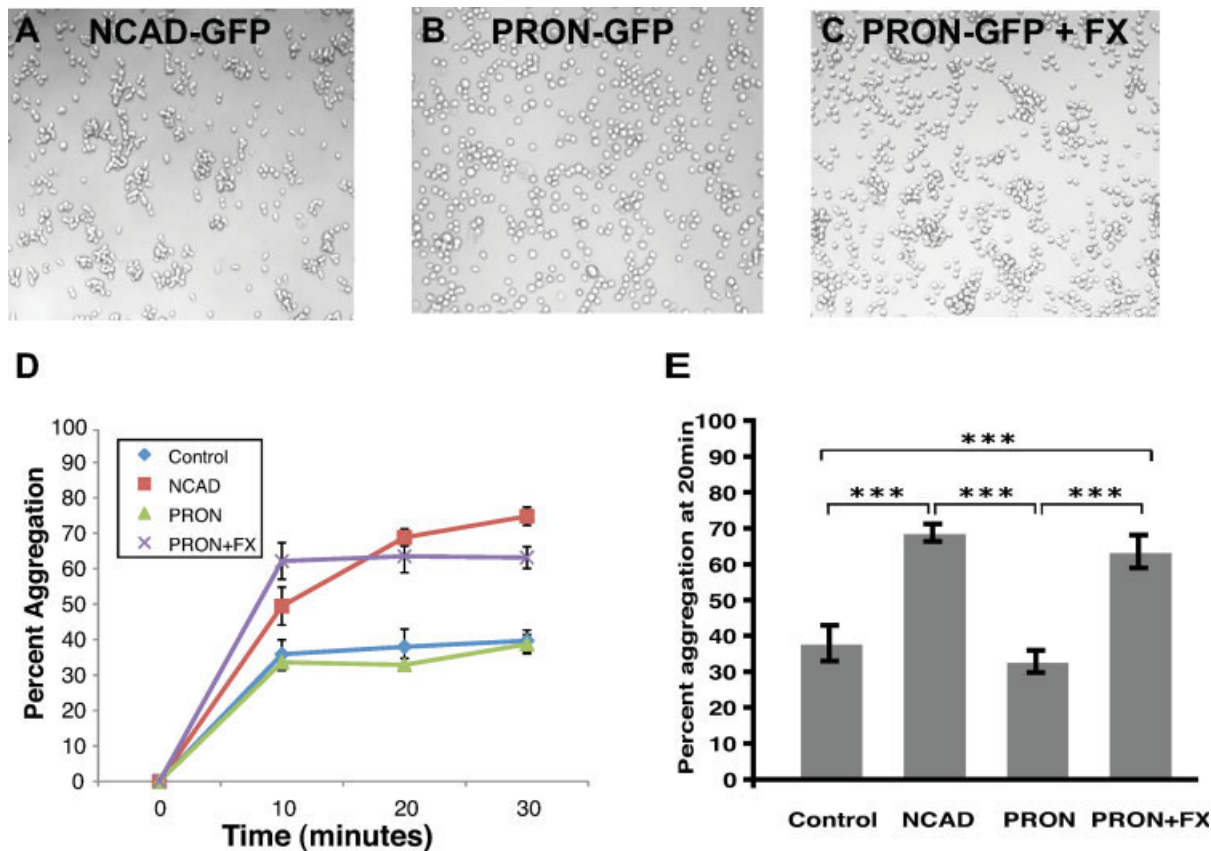


**Figure 4** The prodomain of zebrafish N-cadherin prevents adhesion. (A–C) L-cells in suspension expressing either NCAD-GFP (A), PRON-GFP (B), or PRON-GFP treated with factor Xa to cleave off the pro-domain (C). L-cells expressing PRON-GFP aggregate less than cells expressing NCAD-GFP or Factor Xa-treated PRON-GFP cells. (D) Changes in percent aggregation with time for the various conditions. (E) Comparison of aggregation after 20 min in suspension.  $N \geq 6$  for all conditions.  $N^{***} p < 0.001$ , ANOVA with Bonferroni post-test. Error bars are SEM. [Color figure can be viewed in the online issue, which is available at [www.interscience.wiley.com](http://www.interscience.wiley.com).]

when held in suspension. Cells expressing NCAD-GFP exhibited an appreciable level of aggregation, reaching double that of control cells after 20 min [Fig. 4(A,D)]. In contrast, cells expressing PRON-GFP had an aggregation rate similar to control cells. When PRON-GFP expressing cells were treated with Factor Xa, to cleave off the prodomain [Fig. 2(A)], their level of aggregation approached that of cells expressing NCAD-GFP. By 20 min both NCAD-GFP and Factor Xa-treated PRON-GFP expressing cells aggregated more than untreated PRON-GFP expressing cells, which were no different from control cells [Fig. 4(E)]. We verified that the levels of NCAD-GFP and PRON-GFP expression in L-cells expressing either construct were comparable by measuring relative fluorescence intensities and also confirmed by western blot analysis that cleavage of the prodomain was occurring in L-cells expressing NCAD-GFP and in L-cells expressing PRON-GFP when they were

treated with factor Xa (data not shown). Thus, zebrafish N-Cadherin shows greatly reduced adhesivity prior to cleavage of its prodomain.

### N-Cadherin Adhesivity Regulates Synapse Formation in Rohon-Beard Neurons

It has been proposed that synaptic adhesion molecules facilitate the formation and stability of synapses. To investigate whether the adhesivity of N-cadherin expressed along the Rohon-Beard axon modulates synaptogenesis, embryos expressing NCAD-GFP, PRON-GFP, or DsRed, were fixed and stained for SV2 and PSD95 by wholemount immunohistochemistry [Fig. 5(A)]. A quantitative analysis of NCAD-GFP puncta in 24–36 hpf larvae revealed that  $77.5\% \pm 5.7\%$  of puncta colocalized with SV2 and  $66.5\% \pm 7.2\%$  of NCAD-GFP puncta colocalized



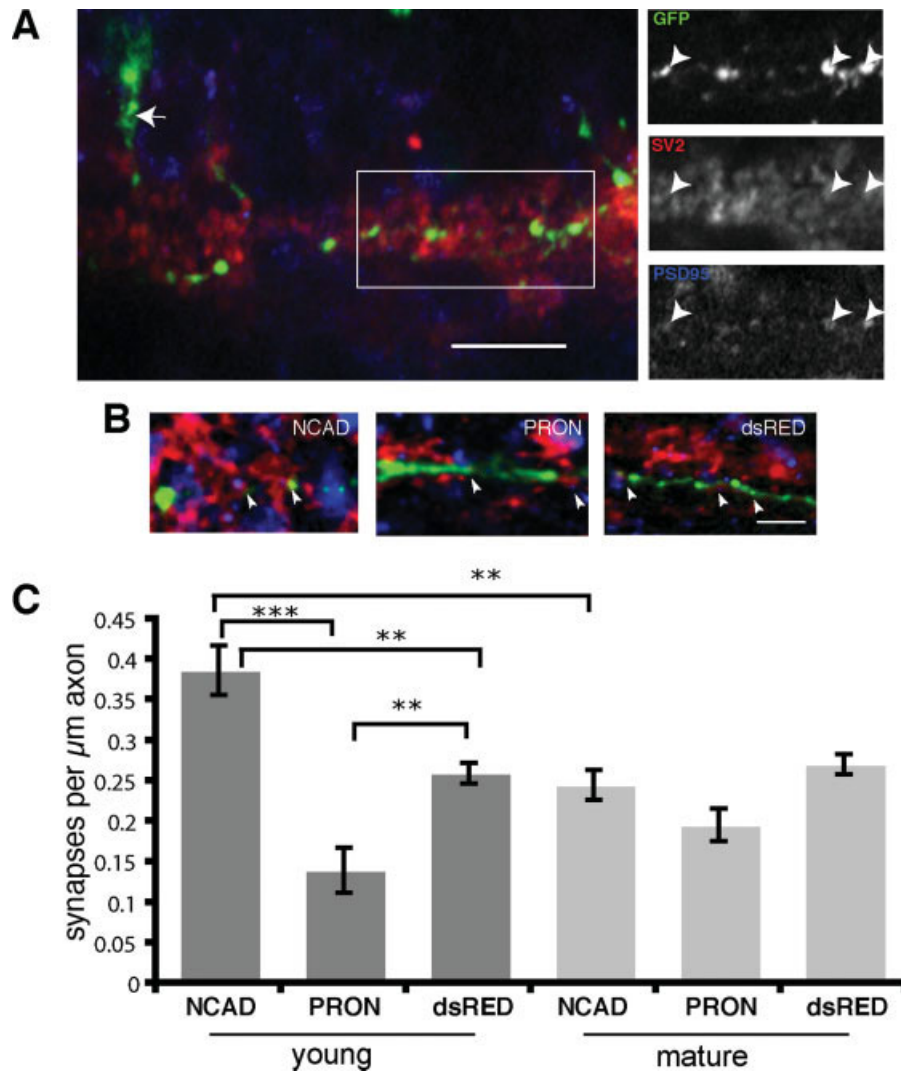


**Figure 5** Transient increase of synapse density with NCAD-GFP overexpression and decrease with PRON-GFP expression. (A) Wholemount immunohistochemistry was performed on zebrafish embryos expressing NCAD-GFP, PRON-GFP, or DsRed in Rohon-Beard neurons. All images are single confocal optical sections taken after triple-labeling a young (30 hpf) embryo with antibodies against GFP, SV2, and PSD95 to visualize transfected neurons, presynaptic, and postsynaptic sites, respectively. A region of the image (rectangle) highlighting the central neuropil of the Rohon-Beard axon is displayed as individual fluorescence channels to the right. Arrowheads indicate examples of putative synaptic puncta. (B) Example segments of NCAD-GFP, PRON-GFP, or DsRed expressing axons (green) immunostained for synapse counting based on juxtaposition of SV2 (red) and PSD95 (blue). (C) Quantitative analysis of putative synapse density along central Rohon-Beard axons in young (24–36 hpf) and mature (36–60 hpf) embryos reveals a transient acceleration of synaptogenesis in cells overexpressing NCAD-GFP and a delay in cells expressing PRON-GFP compared with DsRed controls. Scale bar is 10  $\mu\text{m}$ .  $N = 11$  young NCAD, 12 young PRON, 8 young DsRed, 4 mature NCAD, 5 mature PRON, and 6 mature DsRed expressing neurons.  $**p < 0.01$ ,  $***p < 0.001$  ANOVA with Bonferroni post-test. Error bars are SEM.

with SV2 directly adjacent to a PSD95 punctum, consistent with previous reports that N-cadherin accumulates at synapses (Benson and Tanaka, 1998; Miskovich et al., 1998; Togashi et al., 2002). In subsequent analyses we considered only those SV2 positive

puncta that were found in direct juxtaposition to a PSD95 positive punctum as putative synapses. The density of synaptic puncta along transfected axons overexpressing NCAD-GFP, PRON-GFP, or DsRed was counted in three-dimensional reconstructions

made from confocal images of immunostained wholemount larvae [Fig. 5(B)]. In young (24–36 hpf) neurons, over-expression of PRON-GFP greatly reduced the density of synapses. Young, PRON-GFP over-expressing neurons had  $0.14 \pm 0.01$  synapses per  $\mu\text{m}$  axon compared with DsRed expressing control neurons which had  $0.26 \pm 0.03$  synapses per  $\mu\text{m}$  axon. Conversely, NCAD-GFP over-expression increased the density of synapses made in young neurons ( $0.38 \pm 0.03 \mu\text{m}^{-1}$ ) by 46% [Fig. 5(C)]. Interestingly, by 36 hpf the numbers of synapses in NCAD-GFP expressing neurons and PRON-GFP expressing neurons were no longer significantly different and the number of synapses in each group approached that in control cells expressing DsRed.

## DISCUSSION

This study provides evidence that regulated cleavage of the N-cadherin prodomain participates in its proper targeting in axons and that during development uncleaved Pro-N-cadherin is present in axons where it is able to regulate the rate of formation of synapses. Little is known about the cell biological mechanisms by which N-cadherin is targeted to the cell surface and by what processes it influences synapse formation. Biochemical evidence suggests that N-cadherin is a constituent of presynaptic transport vesicles that may be delivered directly to developing synaptic sites (Zhai et al., 2001). *In vivo* time-lapse data support a model in which it is transported to microdomains associated with synapses by vesicular trafficking (Jontes et al., 2004). The diffuse distribution of PRON-GFP that we observed is most likely a direct consequence of the inability of N-cadherin bearing its prodomain to integrate into stable adhesive contacts. The cleavage of the N-cadherin prodomain normally permits N-cadherin monomers to form cis-dimers and lateral clusters which would then facilitate intercellular trans-dimer interactions. In this way, NCAD-GFP can become spatially restricted into puncta at cell-cell contact points like synapses. Consistent with the ongoing aggregation of N-cadherin into clusters, we noticed a loss of smaller puncta as Rohon-Beard cells matured, which appeared to be accompanied by the fusion of small motile puncta into larger domains. Because the prodomain of PRON-GFP cannot be cleaved, cis-dimers, lateral clusters and transdimers never form and the construct can therefore diffuse freely along the axon. Our observation that endogenous PRON is present along the axons of developing Rohon-Beard neurons suggests a model in which immature pro-N-cadherin is delivered to the cell sur-

face, possibly via presynaptic transport vesicles together with mature N-cadherin, to regulate the kinetics of synaptic adhesion and possibly to be cleaved on demand to rapidly enhance synaptic adhesion and synapse assembly.

Western blot analysis, using an antibody to the N-cadherin prodomain, revealed a band at 150 kD (expected size for full length cadherin containing its prodomain) and a band at 20 kD (expected size for the cleaved prodomain) [Fig. 1(A)]. In the adult zebrafish brain, N-cadherin is present in both its immature pro-form and its mature, cleaved form. It is noteworthy that the cleaved prodomain is fairly plentiful in western blots. In addition to being a byproduct of immature N-cadherin cleavage, the released prodomain may also serve an independent signaling role.

Prodomains of members of the associated disintegrin and metalloprotease (ADAM) family of proteolytic enzymes have been shown to be biologically active in their soluble forms (Wewer et al., 2006; Moss et al., 2007). In particular, the soluble prodomain of ADAM10 whose substrates include epidermal growth factor, Notch, and Amyloid precursor protein, has been shown to act as a competitive inhibitor of the ADAM10 catalytic/disintegrin domain. ADAM10 is responsible for the constitutive and regulated cleavage of N-cadherin in fibroblasts and neuronal cells, directly reducing the overall level of N-cadherin expression at the surface (Reiss et al., 2005). Also, membrane type 5 matrix metalloprotease (MT5-MMP) was shown to both interact with AMPA receptors and to cleave N-cadherin in neurons (Monea et al., 2006).

It is revealing that with development, Rohon-Beard neurons seem to compensate for the extra synapses formed as a result of NCAD overexpression and for the dominant negative effect of PRON overexpression on synapse number. By 2 days post-fertilization, the number of synapses in NCAD expressing Rohon-Beard cells decreased dramatically when compared with one day post-fertilization and the number of synapses in PRON expressing neurons increased dramatically when compared with 1DPF, both reaching levels close to control axons. It is compelling to speculate that neurons may have mechanisms to regulate synapse number at an ideal set point. Previous work suggests that N-cadherin may have a role in this regulation early in development, as inactivation of classical cadherins in young neurons inhibited synapse formation (Togashi et al., 2002), but when neurons reach maturity, cadherins become dispensable for orchestrating the alignment of pre and postsynaptic proteins and the development of synapses (Bozdagi et al., 2004). Nectins, a small family of Ig domain proteins,

may associate with cadherins in the regulation of synapse formation. Nectins distribute asymmetrically at synapses, promote the recruitment of cadherins to points of cell-cell contact in non-neuronal cells (Honda et al., 2003), and have been shown to promote preferential contact between axons and dendrites (Togashi et al., 2006). Also, similarly to N-cadherin, Nectins are initially expressed at both excitatory and inhibitory synapses but during maturation are progressively lost from inhibitory synapses (Lim et al., 2008).

It is possible that as yet unknown interactions with nectins or other molecules regulate signaling to correct for excessive or deficient synapse formation as we observed synapse number approach control levels as neurons mature. In addition to interactions with nectins, N-cadherin is known to interact with a variety of other molecules both intracellularly, like catenins, and extracellularly, including integrins, glutamate receptors, and matrix metalloproteases, which are likely to influence its adhesive strength, localization, stability, as well as its delivery to the plasma membrane. Indeed  $\beta$ -catenin has been implicated in the accumulation of presynaptic elements at developing synapses (Bamji et al., 2003, 2006). These assorted interactions may allow for proper targeting and timing of synapse development and may also serve as a system of checks and balances to correct for excessive or insufficient synapse formation.

The authors are grateful to Pierre Drapeau for expert advice on the care, maintenance, embryonic injection, and mating of zebrafish, and for providing zebrafish embryos for injection. The authors are also grateful to Weisong Shan for providing advice and protocols for the adhesion assay. They specially thank David R. Colman for extensive intellectual input and financial support for this project.

## REFERENCES

- Andersen SSL. 2002. Preparation of dissociated Zebrafish spinal neuron cultures. *Methods Cell Sci* 23:205–209.
- Bamji SX, Rico B, Kimes N, Reichardt LF. 2006. BDNF mobilizes synaptic vesicles and enhances synapse formation by disrupting cadherin-beta-catenin interactions. *J Cell Biol* 174:289–299.
- Bamji SX, Shimazu K, Kimes N, Huelsken J, Birchmeier W, Lu B, Reichardt LF. 2003. Role of beta-catenin in synaptic vesicle localization and presynaptic assembly. *Neuron* 40:719–731.
- Benson DL, Tanaka H. 1998. N-cadherin redistribution during synaptogenesis in hippocampal neurons. *J Neurosci* 18:6892–6904.
- Bozdagi O, Shan W, Tanaka H, Benson DL, Huntley GW. 2000. Increasing numbers of synaptic puncta during late-phase LTP: N-cadherin is synthesized, recruited to synaptic sites, and required for potentiation. *Neuron* 28:245–259.
- Bozdagi O, Valcin M, Poskanzer K, Tanaka H, Benson DL. 2004. Temporally distinct demands for classic cadherins in synapse formation and maturation. *Mol Cell Neurosci* 27:509–521.
- Craig AM, Lichtman JW. 2001. Getting a bead on receptor movements. *Nat Neurosci* 4:219–220.
- Fannon AM, Colman DR. 1996. A model for central synaptic junctional complex formation based on the differential adhesive specificities of the cadherins. *Neuron* 17:423–434.
- Fields RD. 2006. Advances in understanding neuron-glia interactions. *Neuron Glia Biol* 2:23–26.
- Galko MJ, Tessier-Lavigne M. 2000. Function of an axonal chemoattractant modulated by metalloprotease activity. *Science* 289:1365–1367.
- Gerrow K, El-Husseini A. 2006. Cell adhesion molecules at the synapse. *Front Biosci* 11:2400–2419.
- Honda T, Shimizu K, Fukuhara A, Irie K, Takai Y. 2003. Regulation by nectin of the velocity of the formation of adherens junctions and tight junctions. *Biochem Biophys Res Commun* 306:104–109.
- Jontes JD, Emond MR, Smith SJ. 2004. In vivo trafficking and targeting of N-cadherin to nascent presynaptic terminals. *J Neurosci* 24:9027–9034.
- Kalus I, Bormann U, Mzoughi M, Schachner M, Kleene R. 2006. Proteolytic cleavage of the neural cell adhesion molecule by ADAM17/TACE is involved in neurite outgrowth. *J Neurochem* 98:78–88.
- Kalus I, Schnegelsberg B, Seidah NG, Kleene R, Schachner M. 2003. The proprotein convertase PC5A and a metalloprotease are involved in the proteolytic processing of the neural adhesion molecule L1. *J Biol Chem* 278:10381–10388.
- Koch AW, Farooq A, Shan W, Zeng L, Colman DR, Zhou MM. 2004. Structure of the neural (N-) cadherin prodomain reveals a cadherin extracellular domain-like fold without adhesive characteristics. *Structure* 12:793–805.
- Lim ST, Lim KC, Giuliano RE, Federoff HJ. 2008. Temporal and spatial localization of nectin-1 and I-afadin during synaptogenesis in hippocampal neurons. *J Comp Neurol* 507:1228–1244.
- Lohmann C, Bonhoeffer To. 2008. A role for local calcium signaling in rapid synaptic partner selection by dendritic filopodia. *Neuron* 59:253–260.
- Miskevich F, Zhu Y, Ranscht B, Sanes JR. 1998. Expression of multiple cadherins and catenins in the chick optic tectum. *Mol Cell Neurosci* 12:240–255.
- Monea S, Jordan BA, Srivastava S, DeSouza S, Ziff EB. 2006. Membrane localization of membrane type 5 matrix metalloproteinase by AMPA receptor binding protein and cleavage of cadherins. *J Neurosci* 26:2300–2312.
- Moss ML, Bomar M, Liu Q, Sage H, Dempsey P, Lenhart PM, Gillispie PA, et al. 2007. The ADAM10 prodomain is a specific inhibitor of ADAM10 proteolytic activity and inhibits cellular shedding events. *J Biol Chem* 282:35712–35721.

- Ozawa M, Kemler R. 1990. Correct proteolytic cleavage is required for the cell adhesive function of uvomorulin. *J Cell Biol* 111:1645–1650.
- Reiss K, Maretzky T, Ludwig A, Tousseyn T, de Strooper B, Hartmann D, Saftig P. 2005. ADAM10 cleavage of N-cadherin and regulation of cell-cell adhesion and beta-catenin nuclear signalling. *Embo J* 24:742–752.
- Shan WS, Tanaka H, Phillips GR, Arndt K, Yoshida M, Colman DR, Shapiro L. 2000. Functional cis-heterodimers of N- and R-cadherins. *J Cell Biol* 148:579–590.
- Sperry RW. 1963. Chemoaffinity in the orderly growth of nerve fiber patterns and connections. *Proc Natl Acad Sci USA* 50:703–710.
- Tamura K, Shan WS, Hendrickson WA, Colman DR, Shapiro L. 1998. Structure-function analysis of cell adhesion by neural (N-) cadherin. *Neuron* 20:1153–1163.
- Tang L, Hung CP, Schuman EM. 1998. A role for the cadherin family of cell adhesion molecules in hippocampal long-term potentiation. *Neuron* 20:1165–1175.
- Togashi H, Abe K, Mizoguchi A, Takaoka K, Chisaka O, Takeichi M. 2002. Cadherin regulates dendritic spine morphogenesis. *Neuron* 35:77–89.
- Togashi H, Miyoshi J, Honda T, Sakisaka T, Takai Y, Takeichi M. 2006. Interneurite affinity is regulated by heterophilic nectin interactions in concert with the cadherin machinery. *J Cell Biol* 174:141–151.
- Vaughn JE. 1989. Fine structure of synaptogenesis in the vertebrate central nervous system. *Synapse* 3:255–285.
- Wewer UM, Morgelin M, Holck P, Jacobsen J, Lydolph MC, Johnsen AH, Kveiborg M, et al. 2006. ADAM12 is a four-leafed clover: The excised prodomain remains bound to the mature enzyme. *J Biol Chem* 281:9418–9422.
- Yamagata M, Sanes JR, Weiner JA. 2003. Synaptic adhesion molecules. *Curr Opin Cell Biol* 15:621–632.
- Zhai RG, Vardinon-Friedman H, Cases-Langhoff C, Becker B, Gundelfinger ED, Ziv NE, Garner CC. 2001. Assembling the presynaptic active zone: A characterization of an active one precursor vesicle. *Neuron* 29:131–143.
- Ziv NE, Garner CC. 2004. Cellular and molecular mechanisms of presynaptic assembly. *Nat Rev Neurosci* 5:385–399.